Supporting Information

Manning and Peterson 10.1073/pnas.1420096111

SI Materials and Methods

Protein Purification. Tandem affinity purification of SWI/SNF, RSC, SWI/SNF–Δ10R, and Sir2p/Sir4p was performed as described (1, 2). FLAG purification of Isw2 and Sir3p was performed as described for Sir3p-FLAG (2), except that 350 mM NaCl (no KCl) was used during the entire purification and that following elution with 3× FLAG peptide, the protein was concentrated to ∼3μM with a 10,000 polyethersulfone (PES) molecular weight cutoff Vivaspin 500 concentrator (Sartorius; no. VS0101). Concentrated Sir3p was dialyzed (Pierce; no. 69570) for 2 h at 4 °C into storage buffer [20 mM Hepes, pH 7.5, 80 mM NaCl, 10% (vol/vol) glycerol, 0.1% Tween 20] and frozen in liquid nitrogen.

Concentrations of Sir3p and Sir2p/4p were calculated by ImageJ quantification (imagej.nih.gov/ij/) of Coomassie-stained SDS/PAGE gel image intensities, using purified fraction V BSA for known protein mass standards. Concentration of active chromatin-remodeling enzyme was calculated by measuring rates of ATP hydrolysis (see below) at saturating concentrations of dsDNA nucleic acid cofactor. These ATPase concentrations and Sir2p/Sir4p concentrations were used to load equimolar amounts of protein for SDS/PAGE analysis. Silver stain, immunodetection of Arp9p (for RSC and SWI/SNF), and immunodetection of the TAP tag resulted in intensities that were equivalent between complexes.

GST fusion proteins were expressed by using the pGEX-3X vector in Rosetta 2 BL-21 (DE3) cells (EMD; no. 71397). *Escherichia coli* were grown at 28 °C to an OD_{600} of 0.5, in 50 mL of LB with 50 μg/mL carbenicillin and 17 μg/mL chloramphenicol, and then protein expression was induced by the addition of isopropyl beta-D-thiogalactoside (IPTG) to a final concentration of 0.2 mM. After 1 h of protein expression, *E. coli* were harvested by centrifugation at 2,500 × *g* at 4 °C for 15 min in a Beckman J-6B centrifuge with a JS-4.2 rotor. Cell pellet was stored at −80 °C and then thawed on ice and resuspended in 7.5 mL of lysis buffer [1× PBS (pH 7.4) with 1% Triton, 1 mM DTT, and protease inhibitors (0.17 μg/mL aprotinin, 2 μg/mL leupeptin, 2 μg/mL pepstatin, 100 μg/mL PMSF, and 1 mM benzamidine)]. After transfer to a 40-mL centrifuge tube, cells were lysed via four 15-s pulses of sonication (setting 5; Fisher 550 sonic dismembrator) interspersed with incubations on ice to prevent heat accumulation. Lysed cells were incubated on ice for 15 min and then bacterial debris was removed by centrifugation for 25 min at 27,000 × *g*, at 4 °C in a Beckman J2-HC centrifuge with a JA-17 rotor. Clear supernatant lysate was frozen in liquid nitrogen and stored at −80 °C.

Before each experiment, lysate aliquots were thawed on ice, and volumes of lysate containing equivalent amounts of each fusion protein (judged from lysate SDS/PAGE) were each brought to a final volume of 1.2 mL by the addition of lysis buffer in a 1.5-mL Eppendorf microcentrifuge tube. These lysates were incubated with 15 μL of glutathione Sepharose 4B resin slurry (GE; no. 17-0756-01) at 4 °C on a nutator for 1 h. The resin was washed once in lysis buffer, twice in wash-350 buffer (1× PBS with [NaCl] at 350 mM, 0.1% Tween 20, 1 mM DTT, and 100 μg/mL PMSF) and twice in wash buffer (1× PBS, 0.1% Tween 20, 1 mM DTT, and 100 μg/mL PMSF). Each wash consisted of a 5-min incubation at 4 °C on a nutator with 1 mL of the appropriate buffer. Resin was collected by centrifugation for 2 min at 2,000 × *g*, and supernatant was removed. Fusion protein concentration and purity were verified by SDS/PAGE, as for Sir3p and Sir2p/Sir4p above.

FLAG-fusion domains were purified from *E. coli* in a manner similar to GST fusion proteins, except postclarification lysate was directly incubated with M2 anti-flag affinity resin (Sigma; A2220). Once the resin was washed, protein was eluted with 0.2 mg/mL 3× FLAG peptide (Sigma; F4799) in 1× PBS. Fusion protein concentration and purity were verified by SDS/PAGE, as described above.

Analysis of Enzyme ATP Hydrolysis Kinetics. ATP hydrolysis assays were performed as described (3), except that quantification of images was performed by using ImageJ (*Radiolabeled Gel and TLC Plate Quantification*). For experiments to measure enzyme K_m, 10 nM enzyme was used. As a nucleic acid cofactor, supercoiled pUC19 (NEB; no. N3041S) plasmid DNA was present, at appropriate concentrations of calculated 200-bp DNA equivalent (13.43 per 2,686-bp plasmid). Microsoft Excel 2010 linear regression was used to calculate the initial velocity of each ATP hydrolysis reaction. This velocity was plotted as a function of 200-bp-mer concentration via Graphpad Prism (Version 6). Nonlinear fitting to the Michaelis–Menten equation yielded V_{max} and K_m parameters. Experiments were performed in triplicate, and error bars represent sample SD.

Chromatin Reconstitution and Remodeling Assays. Recombinant *Xenopus laevis* H2A, H2AS113C, H2B, H3, and H4 histones were expressed from pET vectors in BL-21(DE3) *E. coli*. Histones were purified and reassembled into octamers as described (4). Octamer containing H2AS113C was biotinylated as described (5), and biotinylation was confirmed by Western blot analysis with HRP–Streptavidin. Histone octamers were reconstituted onto purified template DNA by the step salt dialysis method (6) at a nucleosome positioning sequence (NPS) to octamer molar ratio of ∼0.94–1.0. For biotinylated chromatin, one-sixth of the octamer added to the reconstitution contained biotinylated H2AS113C—the rest of the octamer was wild type. After reconstitution, a fraction of each array was digested with EcoRI and electrophoresed on a 4% (wt/vol) Native PAGE gel, in 0.5× TBE buffer (pH 8.0), to resolve nucleosomal and free DNA and estimate nucleosomal saturation.

Milligram quantities of 208-11 and 208-12 *L. variegatus* 5S NPS array-containing plasmid DNA (CP589 and CP426, respectively) were purified from *E. coli* (QIAGEN; no. 12191). DNA was digested with a combination of HhaI, NotI, and HindIII restriction enzymes, and the array DNA molecule was subsequently separated and purified via a 120-mL Sephacryl S-500 gel filtration column (GE; no. 17-0613-01). The 282-bp–Mid601 DNA was amplified via PCR by using Taq polymerase (NEB; no. M0273L) from plasmid pGEM-3Z lower strand 601 (CP1024) using primers GATCCTCTAGAGTCGGGAGCTC and TGACCAAGGAAAGCATGATTCTTCAC. DNA was purified by phenol/chloroform extraction and ethanol precipitation and then digested with XbaI restriction endonuclease. The 208-11 array DNA and 282-bp–Mid601 DNA were radiolabeled by an end fill-in reaction using Klenow Fragment (NEB; no. M0212S) with alpha-^{32}P dCTP and then purified by phenol/chloroform extraction and G-25 resin spin columns.

Mononucleosome sliding assays were performed in 25 mM Hepes, pH 7.5, 50 mM NaCl, 5 mM $MgCl_2$, 0.05% Tween 20, 1 mM ATP, 1% glycerol, 100 μg/mL BSA, and 1 mM DTT. Given amounts of chromatin-remodeling enzyme were incubated with 12 nM 282-bp–Mid601 mononucleosome at 30 °C for 10 min. To stop the reaction, 10 μL of the reaction was added to 2.4 μL of stop buffer [50 mM EDTA, 20% (vol/vol) glycerol, 1 mg/mL supercoiled plasmid DNA], mixed, and quenched on ice. These quenched aliquots were subjected to native PAGE for 45 min at

120 V, in a 4% (wt/vol) gel, in 0.5× TBE. Before visualization, these gels were dried under vacuum for 45 min at 80 °C on a Bio-Rad gel dryer (model 583).

Restriction enzyme accessibility assays were performed as described (7), except that 0.5 U/mL SalI-HF (NEB; no. R3138T) was used in place of HincII enzyme and that 5 nM chromatin-remodeling enzyme and 1.25 nM radiolabeled 208-11 array were used. After phenol/chloroform extraction, cut and uncut DNA were separated by electrophoresis in a 1% agarose gel. Before visualization, these gels were dried under vacuum for 90 min at 60 °C.

Radiolabeled Gel and TLC Plate Quantification. Dried TLC plates, acrylamide gels, and agarose gels were exposed to Molecular Dynamics storage phosphor screens (generally, 3 h for ATPase assays and overnight for mononucleosome sliding or restriction enzyme accessibility assay gels). The screens were scanned on a Storm 820 scanner and then quantitated in ImageJ after processing with the Linearize GelData plugin (rsb.info.nih.gov/ij/plugins/linearize-gel-data.html). For ATPase assays, intensity of free phosphate signal was measured and normalized to the sum of free phosphate plus unhydrolyzed ATP signal. For mononucleosome sliding assays, the intensity of the band corresponding to a centrally positioned nucleosome was measured and normalized to whole-lane intensity. For restriction enzyme accessibility assays, intensity of uncut array DNA signal was normalized to the sum of cut and uncut DNA signal. Experiments were performed in triplicate, and error bars represent sample SD.

Sir3 Eviction Assay. A concentration of 8 nM biotinylated nucleosomal array (96 nM nucleosomes) was incubated with 96 nM Sir3p (unless experimentally varied) in binding buffer (25 mM Hepes, pH 7.5, 50 mM NaCl, 1.75 mM $MgCl_2$, 0.05% Tween 20, 1 mM DTT) for 25 min at 22 °C. Then, an equal volume of 2× enzyme mix (double concentration of chromatin-remodeling enzyme listed in Fig. 4*E*; 2 mM Mg·ATP, 25 mM Hepes, pH 7.5, 100 mM NaCl, 1.75 mM $MgCl_2$, 0.05% Tween 20, 1 mM DTT) was added, and the reaction proceeded for 10 min at 22 °C.

This reaction was then incubated with 10 μg/μL Streptavidin-coated magnetic beads (Invitrogen; catalog no. 11205D) for 5 min at 22 °C. The magnetic beads had been washed twice in pull-down buffer and blocked for 15 min at 22 °C in pull-down buffer supplemented with 100 μg/mL BSA. During blocking and array binding, beads were kept continually suspended by constant rotation. After binding the array to beads, the beads were magnetically captured and the supernatant "unbound" fraction was removed. The beads were resuspended in 1× SDS/PAGE sample buffer, heated for 5 min at 95 °C, and care was taken to magnetically extract the stripped beads from the supernatant "bound" fraction. These fractions were subjected to SDS/PAGE and electroblotted onto nitrocellulose membrane. Sir3 was immunodetected by HRP–FLAG (Sigma-Aldrich; catalog no. A8592) immunoblotting, and H3 was detected by immunoblotting with Abcam antibody no. 1,791. For quantification, the blot in ECL was photographed on a Fujifilm LAS 3000 CCD apparatus and quantified with ImageJ by using the ISAC plugin (rsb.info.nih.gov/ij/plugins/isac.html). Experiments were performed in triplicate, and error bars represent sample SD.

Protein Capture Assays. A total of 2–10 μg of resin-bound protein (equal masses were used of all proteins within the same experiment) of Sir3p–FLAG (on anti-FLAG resin, from right after the wash steps in the purification protocol), SWI/SNF (on calmodulin affinity resin), or recombinant GST fusion protein (on glutathione Sepharose resin) was incubated with 20 μL of free partner protein (20 nM SWI/SNF, RSC, or ISW2; 100 nM Sir3; ~100 μM domain flag fusion) in wash buffer (1× PBS with 0.1% Tween 20, 1 mM DTT, 100 μg/mL PMSF) for 30 min at 22 °C with continuous gentle rotation. Resin was washed twice with 200 μL of wash buffer and then resuspended in 12 μL of 1× SDS/PAGE sample buffer, heated to 95 °C for 5 min, centrifuged at 18,000 × *g* in a tabletop microcentrifuge; the resultant supernatant was subjected to SDS/PAGE. These gels were electroblotted onto a nitrocellulose membrane, and equal resin-bound protein loading was confirmed by Ponceau staining. Protein was detected by Western analysis with the denoted antibodies. αArp9p Santa Cruz yN-19 goat polyclonal IgG was used to detect Arp9p in Westerns, and tap-tagged proteins were detected by probing for CBP (Millipore; no. 07-482).

Far Western Assays. ~300 nmol each of each purified complex was subjected to SDS/PAGE and electroblotting via wet transfer onto PVDF membrane. Insufficient protein was loaded to visualize by Ponceau staining, so an identical gel was visualized by silver stain (Life Technologies; LC6070) to confirm that equal amounts of complex were used. Far Western analysis was performed as described (8), with 3 mL of 10 nM purified Sir3p–FLAG solution in 1× PBS and 3mg/mL BSA as the probe solution. Sir3p-bound peptide bands were subsequently detected with HRP-conjugated anti-FLAG antibody (Sigma; no. A8592) and visualized with ECL (Thermo; no. 34087).

Structural Modeling. A predicted structure for the SWI/SNF ATPase domain was created by the Phyre2 protein fold prediction server (www.sbg.bio.ic.ac.uk/phyre2/html/page.cgi?id=index) (9). Protein Data Bank (PDB) files were visualized for figures by using PyMOL (Version 1.3; www.pymol.org/). For structural alignment, crystal structures of *Saccharomyces cerevisiae* (PDB ID code 1M4Z) and *M. musculus* (PDB ID code 4DOV) Orc1 (10, 11) were aligned by using the Research Collaboratory for Structural Bioinformatics PDB Protein Comparison Tool (www.rcsb.org/pdb/workbench/workbench.do?action=menu) and visualized in Jmol (jmol.sourceforge.net/). Orc1 BAH domain sequences were aligned by using EMBOSS Needle (www.ebi.ac.uk/Tools/psa/emboss_needle/), and Snf2p homolog N-terminal ATPase lobes were aligned by using Clustal Omega (www.ebi.ac.uk/Tools/msa/clustalo/).

Plasmids. Plasmid for expressing GST-fusion human Orc1 BAH domain was a kind gift of Or Gozani (Stanford University, Stanford, CA) (11). Molecular cloning via PCR, restriction digestion, plasmid ligation, and transformation into *E. coli* was performed by standard methods. Phusion polymerase was used for PCR amplification during cloning (NEB; no. M0530S). For GST fusion protein cloning, coding sequences were cloned into the BamHI and EcoRI restriction sites on pGEX-3X; recombinant flag-domains were cloned into pET expression vectors. Site-directed mutagenesis was used to generate the HSAΔ10 mutation (Agilent; no. 200523). Oligonucleotides used in cloning are listed in Table S1. For cloning details, Table S2.

Yeast Strains and Genetic Methods. For yeast strains used, see Table S3. Standard genetic methods were used for yeast sporulation and tetrad dissection. One copy of the *SWI2* gene was deleted in a diploid strain by a standard PCR-based method (12).

Yeast transformations were performed by using the lithium acetate/PEG/ssDNA carrier method (13). Oligonucleotides and plasmids used for deletion cassette amplification and deletion confirmation are listed in Tables S1 and S2. Yeast genomic DNA preparations were performed by using the glass bead/phenol method (14). Yeast protein extracts were prepared by the standard TCA/glass beads method. Ab5154 and ab1791 antibodies (Abcam) were used for Western blots to detect Swi2p–auxin-inducible degron (AID) and H3 (input), respectively, according to manufacturer recommendations.

For galactose-induced HO endonuclease expression and mating-type switching assays, cells were incubated in appropriate

lactate/glycerol medium to maintain selective pressure (synthetic URA dropout medium for CY2041 + pGal-HO experiments in Fig. S4*A* and YP otherwise; both contained 3% (vol/vol) glycerol, 2% (vol/vol) lactate, 0.05% dextrose, G418, and medium at pH 6.6). At midlog phase (OD_{600} ~0.4), galactose was added to a final concentration of 2% (vol/vol) to induce HO expression, leading to DSB formation at the *MAT* locus. After 1 h (4 h for *swi2Δ* in the plate-based mating-type switching assay in Fig. S4*C*), glucose was added to a final concentration of 2% (vol/vol) to begin glucose repression of HO transcription. For plate-based mating-type switching, cells were diluted at this point to yield 100–200 colonies per plate (dilution empirically determined) and plated onto YPD. After 5 d of growth at 22 °C, colonies were replica plated onto YPD plates with mating-type tester lawns. After growth overnight at 22 °C, mating plates were replica-plated onto synthetic total dropout plates to score colonies with successful mating events.

For yeast genomic DNA preparations to assay DSB formation and repair kinetics via quantitative PCR (qPCR), samples were taken by collecting ~10^7 cells at the appropriate time intervals and centrifuging them at 2500 × *g* for 5 min, 4 °C, in a Beckman J6-B (JS-4.2 rotor). Cell pellets were washed once with ice-cold dH_2O before storing at −80 °C, until processing as above. For inducible degradation of Swi2p–AID, CY1766 yeast culture was grown at 25 °C in YP–lactate until it reached an OD_{600} of 0.25. At that point, the culture was split in half, and either NAA (dissolved at a concentration of 100 mM in 100% ethanol) was added to a final concentration of 1 mM, or an equal amount of just 100% ethanol was used. After 2 h, galactose was added to induce *MAT* locus DSBs, and the experimental timecourse was started (see above). Once added, cells were kept in 1-NAA throughout the experiment.

For serial dilution spot plate assays, CY57 background yeast cells were cultured to saturation at 30 °C in 5 mL of YPD + G418 (two overnights for *SWI2* and *swi2–Δ10R* cells, three overnights for *swi2Δ* cells). Yeast was diluted to an OD_{600} of 1.0 in sterile dH2O, and serially 4.64-fold diluted six times more. A total of 7 μL of each of these seven dilutions was spotted onto plates of the indicated medium. Where used, raffinose was at 2% wt/vol, galactose was 2% wt/vol, HU was at 50 mM, and antimycin A was at 2μg/mL.

For the silencing establishment assay, single colonies of CY1755 (*swi2Δ TELVR::URA3*) that were freshly transformed with either CP1410 or CP1413 were picked off of transformation plates and streaked out onto SD-URA+G418 plates. Biological replicates were performed from separate CP1410/CP1413 transformant colonies. After 2 d at 30 °C, colonies were picked off the −URA plate and inoculated into SC+G418. Cells were kept at an OD_{600} between 0.05 and 0.60 at 30 °C for 3 d by repeated dilution into fresh, prewarmed SC+G418. Time points were taken during those 3 d by diluting cells to an OD_{600} where 200 μL of the cell dilution yielded ~150–400 colonies when plated on 5-FOA+G418. These dilutions were determined empirically, both for strain and for time since beginning growth in SC+G418 (before five population doublings; undiluted culture was used). Another portion of the cell culture was contemporally diluted 1:3,000 and plated on SC+G418 to count total cells. After 3 d, colonies were counted. The number of colonies for each strain and for each time point was normalized both to dilution (above) and to the number of cells that grew on SC+G418. The experiment was biologically repeated five times, and error bars are sample SD.

For RNR induction, yeast cells were grown to midlog, a 0-h time point was taken, then HU was added to a final concentration of 200 mM. After 2 h, the 2-h time point was taken.

qPCR. Primers were designed with Primer3Plus (primer3plus.com/cgi-bin/dev/primer3plus.cgi) with qPCR server settings enabled, except primers for monitoring *MAT* locus breakage and repair, which were obtained from prior literature (14). Reactions were carried out at 25 U/mL NEB Taq (NEB; no. M0273), in NEB Standard TAQ buffer (10 mM Tris, 50 mM KCl, 1.5 mM $MgCl_2$, pH 8.3 at room temperature) supplemented with an additional 1.5 mM $MgCl_2$, 200 μM of each dNTP, 200 nM of each primer, SYBR Green (Invitrogen S-7563; diluted 1:2,000 from stock into DMSO, then diluted 33.33-fold into reaction), and 50-fold diluted Rox dye (BIO-RAD; no. 172–5858). Thermocycling was performed in an Applied Biosystems 7300 RT-PCR system, using Rox as the passive reference dye. Plates were held at 50 °C for 2 min and then held at 95 °C for 10 min, then cycled 40 times between 95 °C for 15 s and 61 °C for 1 min, and finally subjected to dissociation curve analysis. CT values were obtained via the "auto analyze" feature of the AB 7300 software. Standard curves for each primer pair were used to derive slope and intercept values that were subsequently used to calculate quantities of nucleic acid from CTs. Locus quantities were normalized to the ACT1 quantity for their respective nucleic acid prep. All qPCRs were performed in technical duplicate and averaged to give a value for each biological replicate. Three biological replicates were performed for all experiments, except for supplemental Fig. 5*A*, which was performed in biological duplicate and averaged. All error bars represent SD of the sample calculated from the three biological replicate values.

RNA Isolation. RNA was extracted and purified by the hot phenol method, as described (15), from 10- to 50-mL CY57 background cultures (at OD ~0.4–0.6) grown in YEPD, followed by contaminant DNA removal using RNase-free DNaseI (Ambion; no. 1907). RNA concentration and purity were measured on a Nanodrop spectrophotometer. For qRT-PCR analysis, 100 ng of total RNA was subjected to reverse transcription (Invitrogen; no. 11746) with locus-specific qPCR primers for 30 min at 50 °C, before qPCR as above.

For RNA-seq analysis, three biological replicates each of CY57-background yeast cultures, containing either CP1410 or CP1413, were grown to midlog and processed as above. Each replicate was derived from a different transformant colony. The 25-μg samples of RNA were processed for 90-bp paired-end sequencing by BGI International (HK). Data were filtered to remove adaptors, contamination, and low-quality reads from the raw reads. Each sample yielded 28.8–36.4 million reads. These reads were all mapped to the Ensembl EF4 *Saccharomyces cerevisiae* genome build via Tophat (Version 2.0.9) and Bowtie (Version 2.1.0.0), using Samtools (Version 0.1.18.0). Relative gene expression was quantified by Cufflinks (Version 2.1.1), and the resultant data were visualized by CummeRbund (Version 2.6.1) in R (Version 2.15.1) (all as in ref. 16).

1. Smith CL, Horowitz-Scherer R, Flanagan JF, Woodcock CL, Peterson CL (2003) Structural analysis of the yeast SWI/SNF chromatin remodeling complex. *Nat Struct Biol* 10(2):141–145.
2. Buchberger JR, et al. (2008) Sir3-nucleosome interactions in spreading of silent chromatin in Saccharomyces cerevisiae. *Mol Cell Biol* 28(22):6903–6918.
3. Yang X, Zaurin R, Beato M, Peterson CL (2007) Swi3p controls SWI/SNF assembly and ATP-dependent H2A-H2B displacement. *Nat Struct Mol Biol* 14(6):540–547.
4. Luger K, Rechsteiner TJ, Flaus AJ, Waye MM, Richmond TJ (1997) Characterization of nucleosome core particles containing histone proteins made in bacteria. *J Mol Biol* 272(3):301–311.
5. Swygert SG, et al. (2014) Solution-state conformation and stoichiometry of yeast Sir3 heterochromatin fibres. *Nat Commun* 5:4751.
6. Hansen JC, van Holde KE, Lohr D (1991) The mechanism of nucleosome assembly onto oligomers of the sea urchin 5 S DNA positioning sequence. *J Biol Chem* 266(7):4276–4282.
7. Logie C, Peterson CL (1997) Catalytic activity of the yeast SWI/SNF complex on reconstituted nucleosome arrays. *EMBO J* 16(22):6772–6782.
8. Edmondson DG, Dent SYR (2001) *Current Protocols in Protein Science* (John Wiley & Sons, New York).

9. Kelley LA, Sternberg MJE (2009) Protein structure prediction on the Web: A case study using the Phyre server. *Nat Protoc* 4(3):363–371.
10. Connelly JJ, et al. (2006) Structure and function of the Saccharomyces cerevisiae Sir3 BAH domain. *Mol Cell Biol* 26(8):3256–3265.
11. Kuo AJ, et al. (2012) The BAH domain of ORC1 links H4K20me2 to DNA replication licensing and Meier-Gorlin syndrome. *Nature* 484(7392):115–119.
12. Goldstein AL, McCusker JH (1999) Three new dominant drug resistance cassettes for gene disruption in Saccharomyces cerevisiae. *Yeast* 15(14):1541–1553.
13. Schiestl RH, Gietz RD (1989) High efficiency transformation of intact yeast cells using single stranded nucleic acids as a carrier. *Curr Genet* 16(5-6):339–346.
14. Sugawara N, Haber JE (2012) *DNA Repair Protocols, Methods in Molecular Biology*, ed Bjergbæk L (Humana, New York), pp 349–370.
15. Collart MA, Oliviero S (2001) *Current Protocols in Molecular Biology* (John Wiley & Sons, New York).
16. Trapnell C, et al. (2012) Differential gene and transcript expression analysis of RNA-seq experiments with TopHat and Cufflinks. *Nat Protoc* 7(3):562–578.

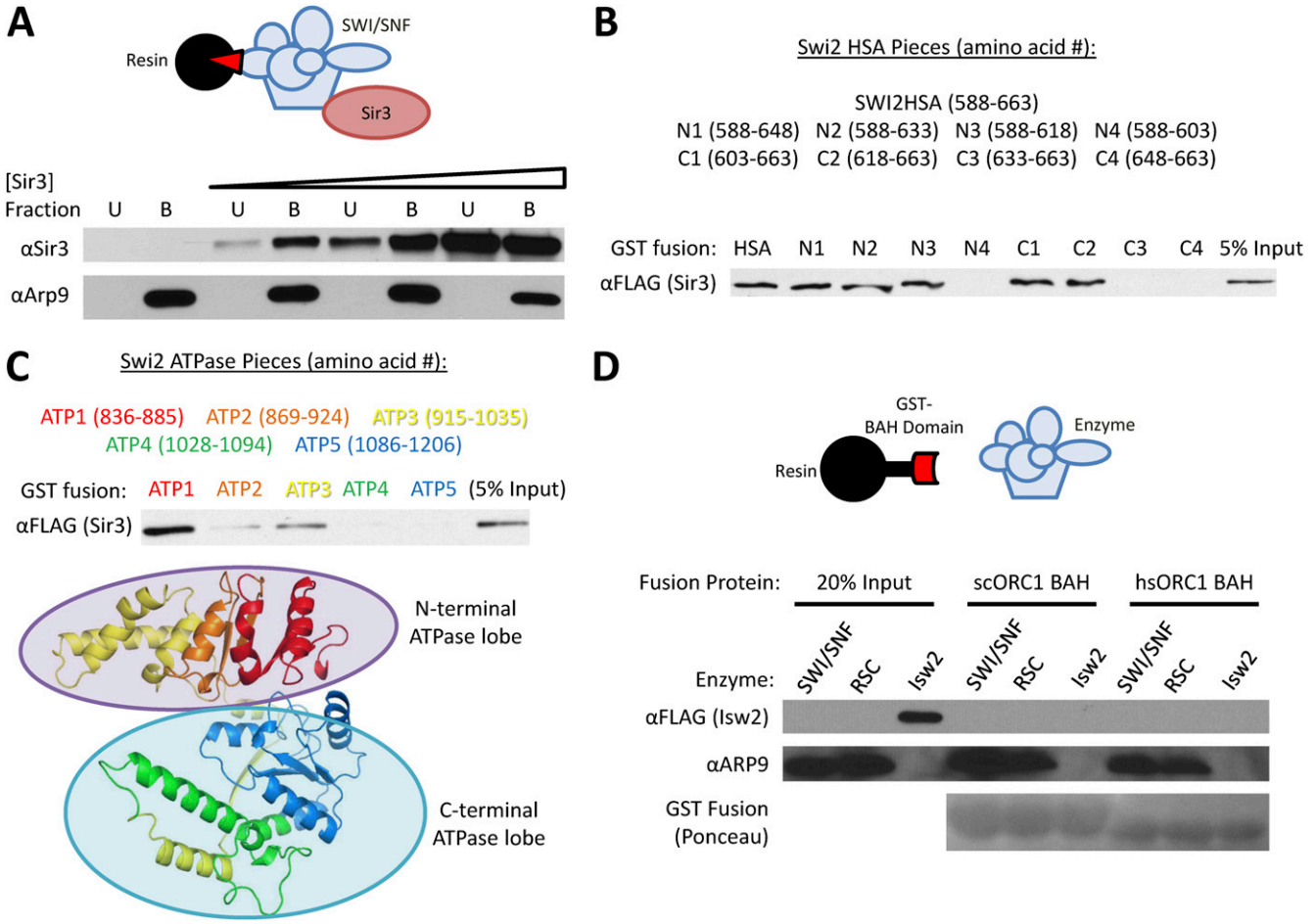

Fig. S1. Characterizing Swi2p subdomains that bind Sir3p. (*A*) Sir3p binds to immobilized SWI/SNF. Calmodulin affinity resin-bound SWI/SNF was incubated with increasing concentrations of Sir3p. (*B*) A central 10-amino-acid stretch of the Swi2p HSA domain is required for Sir3p binding. GST fusions of the Swi2p HSA and progressive N-terminal truncations (C1–C4) and C-terminal truncations (N1–N4) of it were assayed for ability to bind Sir3p. (*C*) The N-terminal lobe of the Swi2 ATPase is able to bind Sir3p. (*Upper*) Pieces of the Swi2p ATPase were assayed as GST fusions for ability to interact with free Sir3p. (*Lower*) Phyre2 predicted structure (www.sbg.bio.ic.ac.uk/phyre2/html/page.cgi?id=index) of the Swi2p ATPase domain, with different colors representing the corresponding regions of the ATPase domain. (*D*) SWI/SNF and RSC complexes interact with *H. sapiens* Orc1 BAH domain.

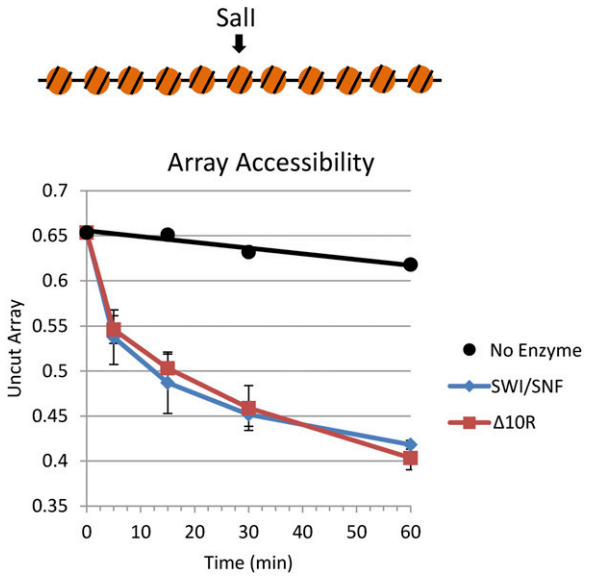

Fig. S2. SWI/SNF–Sir3p contact disruption does not influence array remodeling. SWI/SNF and SWI/SNF–Δ10R were assayed for nucleosome array remodeling activity via the restriction enzyme accessibility assay. Experiment was done in triplicate; error bars denote sample SD.

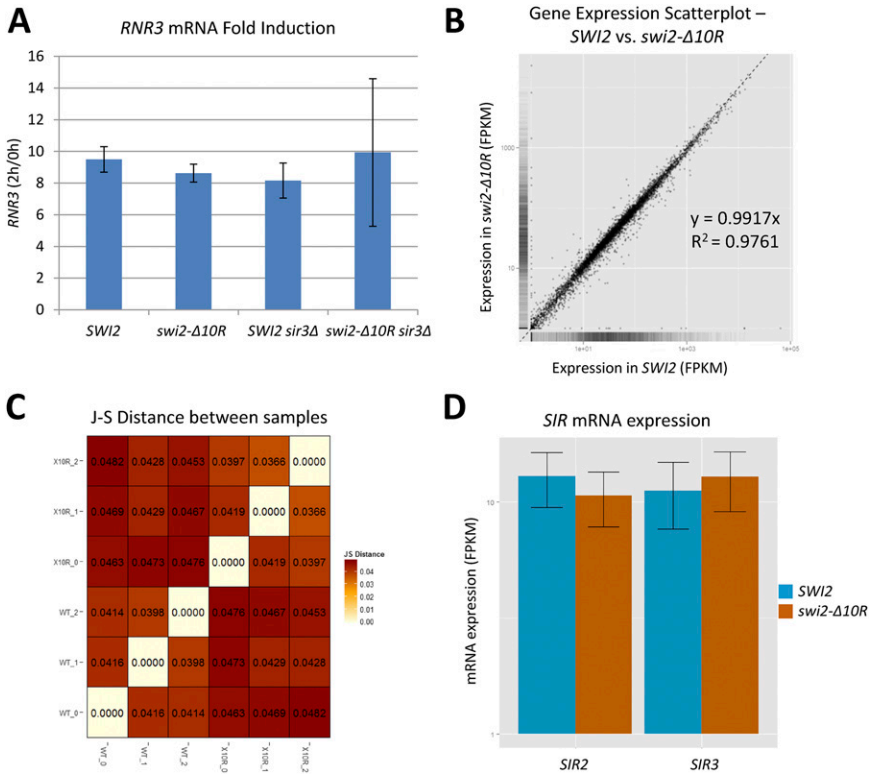

Fig. S3. *swi2–Δ10R* has no major transcriptional effects. (*A*) A *swi2Δ* strain, harboring either *SWI2* (CP1410) or *swi2–Δ10R*(CP1413), and with or without *SIR3* (labels as in Fig. 5*A*), was exposed to 200 mM HU. Expression of *RNR3* relative to *ACT1* expression in each strain was quantified by RT-qPCR before and after exposure to HU. Experiment was done in biological triplicate; error bars represent sample SD. (*B*) Scatterplot of gene expression in *SWI2* and *swi2–Δ10R* as measured by RNA-seq. Each gene is represented by a point. (*C*) Jensen–Shannon distance between *SWI2* and *swi2–Δ10R* RNA-seq replicates. (*D*) *SIR2* and *SIR3* transcript levels are not affected in the *swi2–Δ10R* mutant strain.

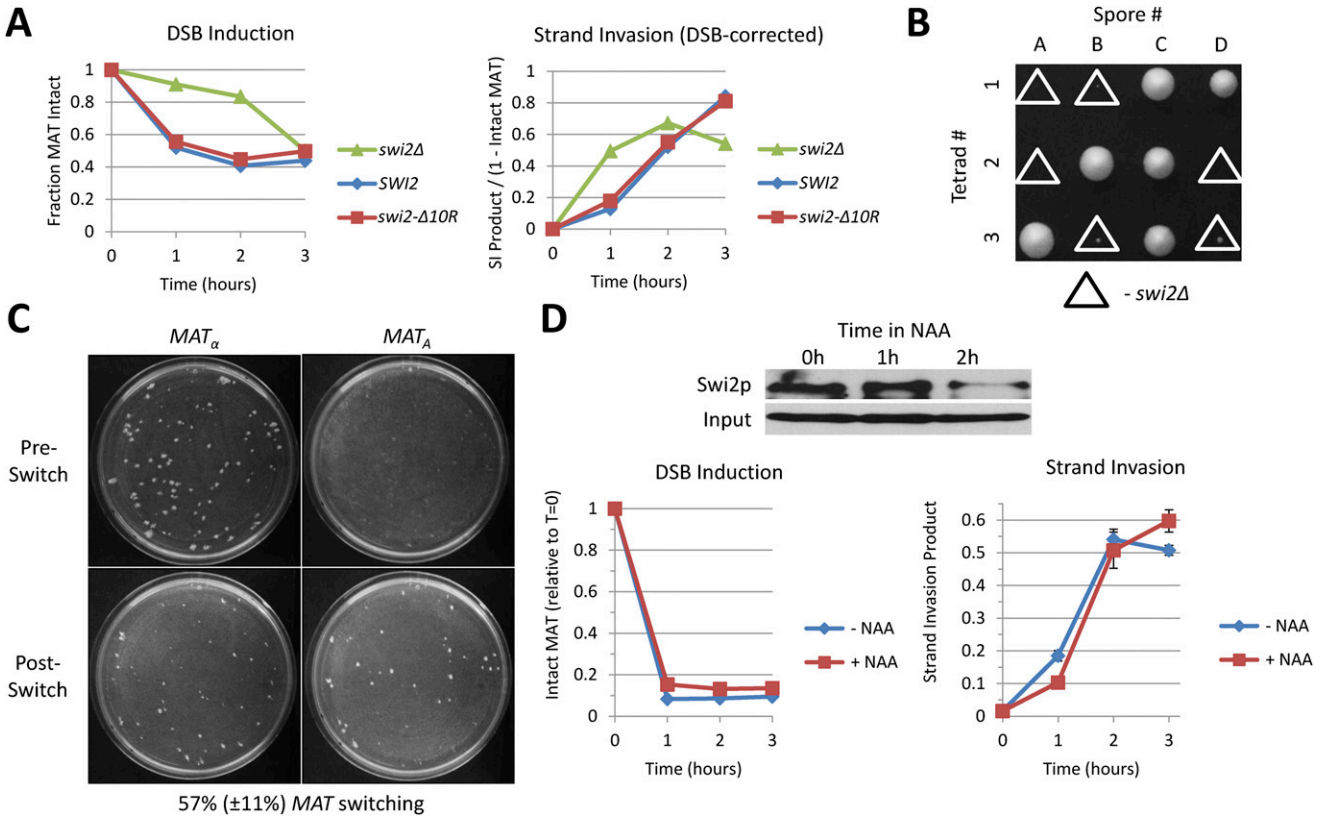

Fig. S4. *SWI2* is dispensable for yeast mating-type switching. (*A*) *swi2Δ* yeast (CY2041) were transformed with *pGAL–HO* and pRS410 alone, CP1410, or CP1413. HO endonuclease expression was induced with galactose and then repressed with glucose to allow repair. Kinetics of HO-induced DSB formation and HR strand invasion were measured by qPCR. Averages of biological duplicates are shown. (*B*) Diploid yeast heterozygous for *SWI2* was sporulated, and the resultant tetrads were dissected into haploid spores. Of the spores shown, 1C, 1D, 2B, 2C, 3A, and 3C are *SWI2*; the rest (triangles) are *swi2Δ*. (*C*) *swi2Δ* strains as from *B* were shifted into galactose to induce mating-type switching and then diluted, plated on rich medium, and subjected to mating-type testing. Shown are representative plates where before galactose, all yeast are MAT_α, and after galactose, ~60% of yeast have become MAT_A. (*D*, *Upper*) A time course showing degradation of AID-tagged Swi2p by *Arabidopsis thaliana* Tir1 E3 ligase in the presence of a synthetic auxin analog. (*Lower*) Kinetics of DSB formation and repair. Experiments were performed as in *A*, but galactose was only added after cultures had been treated with or without 1-NAA.

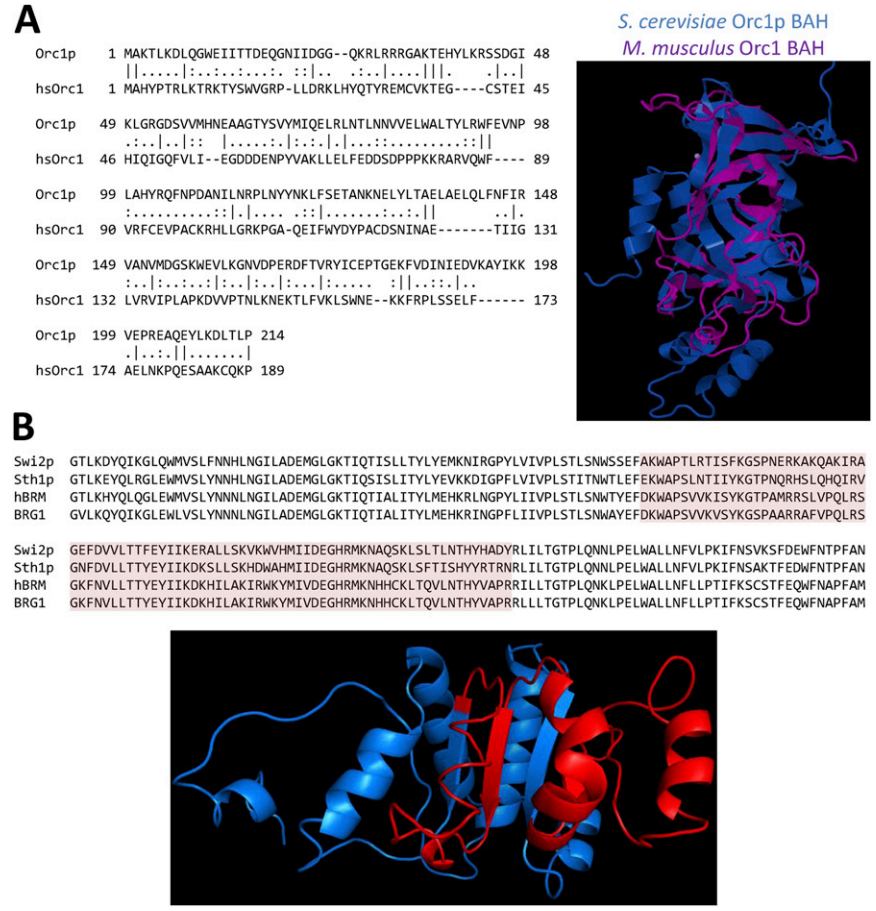

Fig. S5. Conservation of Orc1 BAH domains and SWI/SNF ATPase domains. (*A, Left*) Primary sequence alignment of *S. cerevisiae* Orc1p and *H. sapiens* Orc1 BAH domains. (*Right*) Structural alignment of *Mus musculus* (PDB ID code 4DOV) and *S. cerevisiae* (PDB ID code 1M4Z) Orc1 BAH domains. (*B*, *Upper*) Sequence alignment of the N-terminal ATPase lobes of Snf2p, Sth1p, hBRM and BRG1. (*Lower*) The Snf2p variable region highlighted in red is also colored red in the structural prediction of the Snf2p N-terminal ATPase lobe.

Table S1. Oligonucleotides

Name	Description	Sequence
Making 282bp–Mid601 from CP1024		
282–601MID UP		GATCCTCTAGAGTCGGGAGCTC
282–601MID DOWN		TGACCAAGGAAAGCATGATTCTTCAC
Mating-type confirmation		
MAT DOWN		AGTCACATCAAGATCGTTTATGG
ALPHA UP		GCACGGAATATGGGACTACTTCG
A UP		ACTCCACTTCAAGTAAGAGTTTG
HML DOWN		TGGAACACAGAAAAGAGCAGTG
HMR DOWN		GATTAAGAGAAAATGTCACTACA
MAT qPCR primers		
MAT Down		GGTTAAGATAAGAACAAAGAATGATGCT
DSB MATa UP		CTTTTAGTTTCAGCTTTCCG
SI MATα UP		GCAGCACGGAATATGGGACT
SI MATa UP		GTCGGGTTTTTCTTTTAGTTTCA
ACT1 F		CTTTCAACGTTCCAGCCTTC
ACT1 R		CCAGCGTAAATTGGAACGAC
RNR3 F	MR226	TGAACAAAAGGCGGCATCTG
RNR3 R	MR227	TGTTTCCGTTGGAACTGCTG
Deletion primers		
MR030	Up for *sir3Δ*	TTAAGAAAGTTGTTTTGTTCTAACAATTGGATTAGCTAAAcggatccccgggttaattaa
MR031	Down for *sir3Δ*	CATAGGCATATCTATGGCGGAAGTGAAAATGAATGTTGGTGGGcataggccactagtggatc
MR045	*MX* down	GTATTCTGGGCCTCCATGTC
MR078	*SIR3* 3′UTR R	ACATCTAGTCATTTTGGGTATATTATCGCG
MR079	*SIR3* C term F	TTGTTGTGGTGCTCGAGGAGCCCAGTGC
MR011	Up for *swi2Δ*	TCAGCTATTCTGTTGTTTCTCTAATCGCGACTTTCTGCTATTTTCACGACTTTCGATTAAT-TATCTGCCCGGATCCCCGGGTTAATTAA
MR012	Down for *swi2Δ*	ATAAAAAAAAGAGGGATTAATGTTTGTCTACGTATAAACGAATAAGTACTTATATTGCTTT-AGGAAGGTAGAATTCGAGCTCGTTTAAAC
MR074	*SWI2* 5′UTR F	CCTGAGGCGGTAGGACAATA
MR075	*SWI2* ORF R	TTGCTAAATTGACGCTGTGG
Generating GST fusion proteins		
GST-SIR3BAH-UP		CAGATAGGATCCCCATGGCTAAAACATTGAAAG
GST-SIR3BAH-DOWN		CGGTAGGAATTCCCTGGTACAGATACTCTTTTC
SIR3U1UP		CAGATAGGATCCCCGTGAGTGGGCAGAAGACA
SIR3U1DOWN		CGGTAGGAATTCCCAGATGTCTTCTCTGGCTT
SIR3U2UP		CAGATAGGATCCCCTCACCTACAGATTCTTCG
SIR3U2 DOWN		CTGGGAATTCCAGGTTTTCC
GST-SIR3AAA-UP		CAGATAGGATCCCCAACGCTGATATAAATTTAG
GST-SIR3AAA-DOWN		CGGTAGGAATTCCCTCCGTTAATAGCTTCTGAG
GST-SIR3MID-UP		CAGATAGGATCCCCCCAAAGATGATTGATTTCGC
GST-SIR3MID-DOWN		CGGTAGGAATTCCCCAATTCATTCTTGTCCACC
GST-SIR3END-UP		CAGATAGGATCCCCAAGAACGTAGCCAACGTAAG
GST-SIR3END-DOWN		CGGTAGGAATTCCCTTCATCCATCGAAAAGGCG
SWI2N-UP		CAGATAGGATCCCCAACCGCTGCTATTTAAGA
SWI2N-DOWN		CGGTAGGAATTCCCCGATTCTGTTTGCGTGAT
SWI2HSA-UP		CAGATAGGATCCCCGGTCCATCTAGTGTACAT
SWI2HSA-N-DOWN		CGGTAGGAATTCCCATCGTTCGCCTTTAAAGC
SWI2HSA-C-UP		CAGATAGGATCCCCCATGAATTACTTAAGTTAG
SWI2HSA-DOWN		CGGTAGGAATTCCCCGAAACCATCCACTGTAA
SWI2ATP-UP		CAGATAGGATCCCCGCGAAATGGGCTCCTACC
SWI2ATP-DOWN		CGGTAGGAATTCCCAACTTCATTCTTCTGACC
SWI2C-UP		CAGATAGGATCCCCTCAGTTGAAGAAGTTATC
SWI2C-DOWN		CGGTAGGAATTCCCAGACAAGAAATCATCGTC
SWI2BROMO-UP		CAGATAGGATCCCCAGTGAATTACCTGATATT
SWI2BROMO-DOWN		CGGTAGGAATTCCCCTATACACTCGCTTCTGT
HSAC1 UP		CAGATAGGATCCCCGCCAGATTAAAGTCGATG
HSAC2 UP		CAGATAGGATCCCCAGAAGACAAGATAAAAAG
HSAC3 UP		CAGATAGGATCCCCCTCATTGCTACGCATACT
HSAC4 UP		CAGATAGGATCCCCGCTGAAAAAAAGGCAAAAG
HSAN1 DOWN		CGGTAGGAATTCCCAGCTCTCTTTTGCTCATC
HSAN2 DOWN		CGGTAGGAATTCCCGAGTCTATGGCCAAACTTC
HSAN3 DOWN		CGGTAGGAATTCCCTCTATTATATTGATTGATG
HSAN4 DOWN		CGGTAGGAATTCCCGGCCACTGCCTCAGTCTTC

Table S1. Cont.

Name	Description	Sequence
SWI2ATP2UP		CAGATAGGATCCCCGTTCTGACTACCTTTGAG
SWI2ATP3UP		CAGATAGGATCCCCCATGCAGATTATAGATTA
SWI2ATP4UP		CAGATAGGATCCCCCGTCGTCTTTTTATCGGT
SWI2ATP5UP		CAGATAGGATCCCCGCTGGTAAATTTGAACTA
SWI2ATP1DOWN		CGGTAGGAATTCCCCTTGGATAAAAGTGCTCT
SWI2ATP2DOWN		CGGTAGGAATTCCCACCTGTCAAAATTAATCT
SWI2ATP3DOWN		CGGTAGGAATTCCCACCGATAAAAAGACGACG
SWI2ATP4DOWN		CGGTAGGAATTCCCTCTATCTAATAGTTCAAA
SIR3BAHΔ187DOWN		CGGTAGGAATTCCCAATTGGTACAAACTTTTCCG
SIR3BAHΔ153DOWN		CGGTAGGAATTCCCTATCTGTCCAACTGCAATG
SIR3BAHΔ128DOWN		CGGTAGGAATTCCCTACTTCGTTGAAAAATTTATC
SIR3BAHΔ98DOWN		CGGTAGGAATTCCCTTTGAGTTCAAACCATCTCA
STH1ATP1UP		CAGATAGGATCCCCTGGACTTTAGAATTTGAA
STH1ATP1DOWN		CGGTAGGAATTCCCTTTTGATAAAAGAGATTT
ORC1BAH UP		CAGATAGGATCCCCATGGCAAAAACGTTGAAGG
ORC1BAH DOWN		CGGTAGGAATTCCCCTTTTGAGGACCTCTTTTG
RSC2BAH UP		CAGATAAGATCTCCGATGAAGTCATTGTAAATAATATATC
RSC2BAH DOWN		CGGTAGCAATTGCCGGGGGAAGGATATTTGAAG
RSC2CT1 DOWN		CGGTAGCAATTGCCAAGAGCATTTGCTGTTG
Amplification of FLAG-tagged domains		
SWI2HSAFLAGUP		CAGATACATATGCATGAATTACTTAAGTTAG
SWI2HSAFLAGDOWN		CGGTAGGGATCCTTACTTATCGTCATCGTCTTTATAATCCTTGTCATCGTCATCTT-TGTAGTCATCGTTCGCCTTTAAAGCCTG
BAH-FLAGUP		CAGATACATATGGCTAAAACATTGAAAG
BAH-FLAGDOWN		CGGTAGGGATCCTTACTTATCGTCATCGTCTTTATAATCCTTGTCATCGTCATCTT-TGTAGTCCCCACTCACTGGTACAGA
STH1 ATPase lobe 1 amplification		
STHATP123UP		GATTCGGGTACCTTAAAAGAGTATCAATTACGA
STHATP123DOWN		CACAGGCACCGGTGTTGGCAAATGGAGTATTAAACC
Site-directed mutagenesis of *SWI2*		
SWI2HSA-10 S		CGATGAATAAATCCGCCAAGAATAAAAGGTTG
SWI2HSA-10 AS		CAACCTTTTATTCTTGGCGGATTTATTCATCG
C-terminal TAP tag for CP1414		
TAP–Xho UP		CAGATACTCGAGCATGGAAAAGAGAAGATGGAAAAAG
TAP–Xho DOWN		CGGTAGCTCGAGGTTGACTTCCCCGCGGAATTC

Table S2. Plasmids

ID no.	Backbone	Description
CP126	pGEX-3X	Plasmid for IPTG-inducing expression of N-terminally GST-tagged fusion proteins in DE3 *E. coli*
CP137	YCp50	pGAL–HO; Gal-inducible HO endonuclease expression from YCp50 (GAL10 promoter->HO; CEN/ARS, URA3)
CP337	pRS315	SWI2 in pRS315 (~6300bp Sau3AI-partial piece with ~1kb 5′UTR, ORF, and ~300 bp 3′ UTR)
CP426	pBS SK-	208-12 array; cut out with HhaI to digest backbone
CP589	pBS SK-	208-11 array; cut out with NotI, HindII, and use HhaI to digest backbone
CP717	pET	xH2A expression
CP718	pET	xH2B expression
CP719	pET	xH3 expression
CP720	pET	xH4 expression
CP967	pFA6a	pAG25; for cerevisiae gene deletion cassette template; NatMX4 cassette
CP969	pFA6a	pAG32; for cerevisiae gene deletion cassette template; HphMX4 cassette
CP999	pFA6a	Plasmid for C-terminally tap-tagging
CP1024	pGEM-3z	601 NPS mono plasmid
CP1109	pET	xH2AS113C expression
CP1163	pDM641	pGal1-HA-Sir2/Leu plasmid derived from pRS315
CP1164	pDM654	pGal1-TAP-Sir4/Ura plasmid derived from pRS315
CP1165	pDM1009	pGal1/10-Sir3-FLAG/Leu plasmid derived from pRS425
CP1210	pMK43	C-terminal AID-tag with KanMX
CP1211	pMK76	StuI-Linearizable URA3-integrable AtTIR1
CP1250	pRS410	Yeast CEN/ARS Plasmid; KanMX; Addgene no. 11258
CP1253	pMK43	C-terminal AID-tag with HphMX
CP1406	pRS410	pRS410 cut KpnI–SalI, SWI2 C terminus inserted (CP337 KpnI-SalI)
CP1407	pRS410	CP1406 cut KpnI–AgeI, STH1 ATPase lobe I inserted (aa 468–665; KpnI–SgrAI; 52 divergent aa converted)
CP1408	pRS410	pRS410 cut NgoMIV–KpnI, SWI2 N terminus inserted (CP337 NgoMIV–KpnI)
CP1409	pRS410	CP1408, site-directed mutagenesis HSAΔ10 (aa 613–623 deleted)
CP1410	pRS410	SWI2 in pRS410 CP1408 cut KpnI–SalI, SWI2 C terminus inserted (CP337 KpnI–SalI)
CP1413	pRS410	SWI2 ‘Δ10R’ in pRS410 CP1409 cut KpnI–SalI, STH1-SWI2 chimera ATPase C-term inserted (CP1407 KpnI–SalI)
CP1414	pRS410	CP1407 cut XhoI–BamHI with 4xpA-CTAP inserted (PCR from CP999 with in-frame XhoI inserted; XhoI–BglII)
CP1415	pRS410	SWI2 ‘Δ10R’-TAP in pRS410 CP1414 cut NaeI–AgeI with SWI2 HSA10 N terminus inserted (CP1413 NaeI–AgeI)
CP1416	pGEX-3X	GST-SWI2 N (aa 1–390)
CP1417	pGEX-3X	GST-SWI2 HSA (aa 361–780)
CP1418	pGEX-3X	GST-SWI2 HSAN (aa 316–663)
CP1419	pGEX-3X	GST-SWI2 HSAC (aa 588–780)
CP1420	pGEX-3X	GST-SWI2 ATP (aa 836–1206)
CP1421	pGEX-3X	GST-SWI2 C (aa 1216–1440)
CP1422	pGEX-3X	GST-SWI2 BROMO (aa 1321–1703)
CP1423	pGEX-3X	GST-SWI2 HSA (aa 588–663)
CP1424	pGEX-3X	GST-SWI2 HSAN1 (aa 588–648)
CP1425	pGEX-3X	GST-SWI2 HSAN2 (aa 588–633)
CP1426	pGEX-3X	GST-SWI2 HSAN3 (aa 588–618)
CP1427	pGEX-3X	GST-SWI2 HSAN4 (aa 588–603)
CP1428	pGEX-3X	GST-SWI2 HSAC1 (aa 603–663)
CP1429	pGEX-3X	GST-SWI2 HSAC2 (aa 618–663)
CP1430	pGEX-3X	GST-SWI2 HSAC3 (aa 633–663)
CP1431	pGEX-3X	GST-SWI2 HSAC4 (aa 648–663)
CP1432	pGEX-3X	GST-SWI2 HSAΔ10 (CP1423 with 613–623 deleted)
CP1433	pGEX-3X	GST-SWI2 ATP1 (aa 836–885)
CP1434	pGEX-3X	GST-SWI2 ATP2 (aa 869–924)
CP1435	pGEX-3X	GST-SWI2 ATP3 (aa 915–1035)
CP1436	pGEX-3X	GST-SWI2 ATP4 (aa 1028–1094)
CP1437	pGEX-3X	GST-SWI2 ATP5 (aa 1086–1206)
CP1438	pGEX-3X	GST-STH1 ATP1 (aa 539–588)
CP1439	pGEX-3X	GST-SIR3 BAH (aa 1–214)
CP1440	pGEX-3X	GST-SIR3 U1 (aa 214–350)
CP1441	pGEX-3X	GST-SIR3 U2 (aa 300–440)
CP1442	pGEX-3X	GST-SIR3 MID (aa 460–730)
CP1443	pGEX-3X	GST-SIR3 AAA (aa 530–845)
CP1444	pGEX-3X	GST-SIR3 END (aa 790–970)
CP1445	pGEX-3X	GST-SIR3 BAH1 (aa 1–186)
CP1446	pGEX-3X	GST-SIR3 BAH2 (aa 1–152)
CP1447	pGEX-3X	GST-SIR3 BAH3 (aa 1–127)
CP1448	pGEX-3X	GST-SIR3 BAH4 (aa 1–97)
CP1449	pGEX-3X	GST-ORC1 BAH (aa 1–214)

Table S2. Cont.

ID no.	Backbone	Description
CP1450	pGEX-3X	GST-RSC2 BAH (aa 401–557)
CP1451	pGEX-3X	GST-RSC2 BAHCT-1 (aa 401–642)
CP1452	pET3a	SIR3 BAH-FLAG (aa 1–214)
CP1453	pET3a	SWI2 HSA-FLAG (aa 588–663)

aa, amino acids.

Table S3. Yeast strains

Strain	Source	*MAT*	Genotype
CY57		MAT_{α}	*swi2Δ::*His^{+} *lys2-801*^{A} *ade2-101° trp1-Δ1 his3-Δ200 leu2-Δ1 ura3-52*
CY118		MAT_{A}	*swi2Δ::*His^{+} from CY57 background BUT Trp^{+}
CY384		MAT_{A}	α tester
CY385		MAT_{α}	A tester
CY915	JKM179	MAT_{α}	*Δho Δhml::ADE1 Δhmr::ADE1 ade1–100 leu2,3–112 lys5 trp1::hisG ura3-52 ade3::GAL::HO*
CY924	JKM154	MAT_{A}	*Δho ade1–100 leu2,3–112 lys5 trp1::hisG ura3-52 ade3::GAL::HO*
CY971	W303	MAT_{a}	*swi2Δ::HIS3 leu2-3,112 trp1-1 can1-100 ura3-1 ade2-1 his3-11,15*
CY1274	WDHY668	$MAT_{A/\alpha}$	*ura3-52 trp1 leu2-Δ1 his3-Δ200 pep4Δ::HIS3 prb1-Δ1.6R can1*
CY1496		$MAT_{A/\alpha}$	CY1274 with *[CP1165]*
CY1497		$MAT_{A/\alpha}$	CY1274 with *[CP1163 and CP1164]*
CY1503	BY4741	MAT_{A}	*RSC2-TAP*
CY1504	BY4741	MAT_{A}	*ISW2-FLAG*
CY1552	BY4741	MAT_{A}	*SWI2-TAP*
CY1752	W303	$MAT_{A/\alpha}$	*swi2Δ::HIS3/SWI2 sir3Δ::HphMX/SIR3*
CY1754	L1088	MAT_{A}	*ura3Δ0 leu2Δ0 TEL-VR::URA3*
CY1755	L1089	MAT_{A}	*ura3-52 leu2Δ0 snf2Δ::LEU2 TEL-VR::URA3*
CY1760		$MAT_{A/\alpha}$	CY915 and CY924 mated; *swi2Δ::NatMX/SWI2*
CY1761		MAT_{α}	*swi2Δ::NatMX* segregant from CY1760 with HML_{α} HMR_{A}
CY1762		MAT_{α}	*swi2Δ::NatMX* segregant from CY1760 with HML_{α} HMR_{A}
CY1765		MAT_{A}	CY924 with *URA3::atTIR1* (CP1211 StuI-linearized)
CY1766		MAT_{A}	CY1765 with *SWI2-AID::HphMX*
CY2041			*swi2Δ::HIS3* segregant from CY1752
CY2332		MAT_{α}	CY57 with *sir3Δ::HphMX [CP1410 (SWI2 in pRS410)]*
CY2333		MAT_{α}	CY57 with *sir3Δ::HphMX [CP1413 (Δ10R in pRS410)]*

Dataset S1. RNA-seq gene expression analysis of *SWI2* and *swi2–Δ10R*

Dataset S1